

## Chapter 10: Deep-Seated Oceanic Heat Flow, Heat Deficits, and Hydrothermal Circulation

Robert N. Harris and David S. Chapman

### 10.1. Introduction

The Earth is losing heat at a rate of  $44.2 \times 10^{12}$  W with about 70% occurring through oceanic lithosphere (Pollack et al., 1993). Understanding the magnitude and geographic variation of this heat loss, and the associated physical and chemical processes has been a major pursuit of earth scientists for five decades (e.g., Lee and Uyeda, 1965; Williams and Von Herzen, 1974; Chapman and Pollack, 1975; Jessop et al., 1976; Sclater et al., 1980).

The first order pattern of oceanic heat loss can be explained by the gradual and progressive cooling of lithosphere continuously created at a mid ocean ridge and rafted away from the ridge by sea floor spreading. Cooling of the lithosphere leads to subsidence through thermal contraction and thickening through the accretion of upper mantle material. Mathematical and physical descriptions of this conceptual model are both elegant and simple, providing an explanation of many observations with a limited number of free parameters.

In young oceanic lithosphere, advective heat loss due to crustal hydrothermal circulation is superimposed on the slow conductive heat loss of the lithosphere. Hydrothermal circulation dominates heat transfer where temperature and topographic gradients are sufficient to drive fluid flow, crustal permeabilities are high, and there are open pathways for sea water to enter and exit the oceanic crust. Near the ridge crest and in young sea floor, conditions are ideal for the upper oceanic crust to host vigorous ventilated hydrothermal convection. With the progression of time, temperature gradients and crustal permeability decrease, sediment accumulation isolates the permeable crust from sea water, and heat loss by fluid flow is diminished.

Other than direct venting of high temperature fluids from the seafloor near ridge axes, direct observation of hydrothermal circulation in the crust is difficult. Instead, one infers the presence of fluid flow by measuring the physical or chemical effects of advection and comparing those effects with models. Model sensitivity studies suggest which observations are sensitive to various forms of

hydrothermal convection and show that temperature fields and particularly seafloor heat flow patterns comprise the most diagnostic physical measurements for constraining the nature and vigor of circulation.

Heat flow is the product of the thermal gradient and thermal conductivity, both of which are typically measured in-situ by inserting a gravity-driven heat flow probe into sediments. The requirement for sediment precludes probe measurements on large areas of young seafloor and other bare rock environments where advective heat loss is greatest. Seafloor drilling provides opportunities to measure subsurface temperature fields and thermal blankets (Johnson and Hutnak, 1996) make possible the computation of heat flow in bare rock environments, but the cost of both of these techniques prohibits a spatially dense set of measurements. Once sediment ponds have accumulated on young sea floor, it is physically possible to make heat flow measurements with a probe, but the measurements are often systematically biased. Both observations and theory suggest that sediment ponds tend to be areas of anomalously low heat flow (Chapter 8). Hydrologic recharge and discharge partially occurs through adjacent topographic highs, but the lack of sediments often precludes making measurements to confirm the inference, and focused ventilation in areas of discharge would probably dilute whatever thermal signal might be advected in venting fluids.

Fortunately, both recharge and discharge, do not have to be measured to estimate the magnitude of the advective heat loss. If the deep-seated heat flow is known, then spatially integrated heat flow deficits in areas affected by recharge or lateral flow must match heat flow excesses in discharge areas. Heat flow deficits, in fact, provide important information about the nature and vigor of hydrothermal convection.

While there is general consensus both about the importance of hydrothermal circulation in young oceanic crust and about first order variations of heat flow, sea floor depth, and lithospheric thickness as functions of sea floor age, the details of these processes remain controversial. The recognition that the difference between observed and predicted values of heat flow are largely due to hydrothermal circulation provides a convenient way of estimating the magnitude of advective heat loss through the sea floor and also the flux of water through the oceanic crust (Wolery and Sleep, 1976; Sleep and Wolery, 1978; Stein and Stein, 1994b). However, magnitudes of inferred ridge flank hydrothermal circulation depend in part on the chosen model of lithospheric heat flow which remains contentious. Discussions of advective heat loss also focus on the processes controlling the magnitude and patterns of hydrothermal circulation (Chapter 11) and when fluid flow becomes thermally negligible (Chapter 13). All of these topics remain areas of active investigation.

Thus, the problem confronting the marine hydrologist is to separate the background lithospheric heat flow from the hydrothermal advective heat flow. Strategies for estimating both of these quantities are discussed below and rely on judicious combinations of heat flow and bathymetric data, as well as careful selections of environmentally favorable sites in which to make measurements. The key to these tasks is a clear understanding of each process. The purpose of this chapter is (a) to review models used to predict lithospheric or deep-seated heat flow in oceanic lithosphere, (b) to show how observations are combined with model predictions of heat flow to estimate the magnitude of sea floor hydrothermal convection, and (c) to provide examples of surveys that advance our understanding of hydrothermal circulation in the oceanic crust.

## **10.2. Reference Models for the Thermal Evolution of Oceanic Lithosphere**

Seafloor bathymetry and heat flow provide critical evidence for the thermal state of oceanic lithosphere. These data are complementary in that bathymetry, under conditions of isostatic equilibrium, constrains the integrated temperature structure through the lithosphere while observations of heat flow constrain the shallow temperature regime. Because heat flow observations depend on the thermal gradient at the surface, they are sensitive to shallow thermal processes and are therefore suited to estimating hydrothermal circulation in areas of advective heat flow. In contrast, bathymetry depends primarily on the integrated thermal structure and is better suited to estimating plate scale model parameters. As a result, studies calibrating plate scale thermal models often weight bathymetry more heavily than heat flow (e.g. Davis and Lister, 1974; Parsons and Sclater, 1977; Carlson and Johnson, 1994). A notable exception is the lithospheric model GDH1 (Stein and Stein 1992), which jointly fits both bathymetry and heat flow (on crust older than 55 Ma). Other constraints on the thermal state of oceanic lithosphere such as surface wave velocities, intraplate earthquakes, and flexural thicknesses, are relatively poor quantitative indicators, because the temperature dependence of rheological properties is poorly known. Thus, the combination of seafloor depth and heat flow provides the principal evidence for the thermal evolution of the lithosphere.

Figure 10.1 shows an example of the variation of seafloor bathymetry and heat flow as a function of crustal age. This example (Stein and Stein, 1992) incorporates data from the north Pacific and northwest Atlantic. The depth plot (Figure 10.1a) shows that in general mid ocean ridges are elevated to a depth of 2.5 km and that aging lithosphere ultimately subsides to depths of about 5.5 km. For crust younger than

about 80 Ma the depth increases linearly with the square root of age according to the simple boundary layer cooling (Figure 10.1b) (Parker and Oldenberg, 1973; Davis and Lister, 1974). For older ocean floor, the depth increase tapers off exponentially to an asymptotic value of 5,650 m (Stein and Stein, 1992). However, note that the variability of ocean depth increases with age (Sclater and Wixon, 1986; Renkin and Sclater, 1988). Heat flow also generally decreases as a function of sea floor age, but deviates from model predictions at young ages (Figure 10.1c). Figure 10.1d shows heat flow plotted as a function of the inverse square root of age, the function of time predicted by simple boundary layer cooling (see section 10.2.1). Heat flow is highly variable in young sea floor but, unlike bathymetry, the variability decreases in older sea floor (however, see Chapter 13). These measures of variability may reflect perturbations to the commonly assumed progressive cooling of oceanic lithosphere.

Two classes of models have been proposed to explain these first order observations between bathymetry and heat flow as functions of age. In the half-space model, the lithosphere progressively cools and thickens as it spreads away from the ridge crest (Turcotte and Oxburgh, 1967; Parker and Oldenberg, 1973). The predicted ocean depth is proportional to the square root of age and heat flow decreases inversely with the square root of age. In the plate model, the lithosphere continues to thicken until the geothermal gradient reaches equilibrium and cooling ceases (McKenzie, 1967; Sclater and Francheteau, 1970), presumably as a result of heat being supplied from the asthenosphere at a uniform rate. In this model the predicted ocean depth and heat flow vary exponentially with age. Both of these models are one-dimensional so that horizontal heat conduction is assumed negligible. This assumption holds as long as the width of the plate is large compared to its thickness so that all heat flows in the vertical direction. Additionally, both models assume that heat production is negligible as indicated by heat production measurements of basalt.

### 10.2.1. Half-space model

The half-space model applied to the thermal evolution of oceanic lithosphere refers to a half-space at an initial constant temperature  $T_i$  whose upper boundary temperature is changed to  $T_o$  at time zero and maintained at that temperature. The half-space model has been described elsewhere (e.g., Davis and Lister, 1974) and detailed derivations can be found in many texts (e.g., Turcotte and Schubert, 1982; Fowler, 1990). The temperature,  $T_o$ , is the temperature at the sea floor and is commonly assumed  $0^\circ\text{C}$ . The variation of temperature with depth  $z$  below the seafloor, and age  $t$  is formulated in terms of a step change in surface temperature and given by

$$T(t, z) = T_i \operatorname{erf} \left[ \frac{z}{\sqrt{4\kappa t}} \right] \quad (10.1)$$

where erf is the error function, and  $\kappa$  is thermal diffusivity of the half space. The product of the thermal gradient at  $z=0$  and the thermal conductivity  $\lambda$ , gives the surface heat flow,  $f$ , as

$$f = \lambda T_i / \sqrt{\kappa t}. \quad (10.2)$$

The cooling lithosphere contracts and is loaded by an increasing column of seawater through time. Assuming that the seafloor is regionally in isostatic equilibrium, as indicated by gravity measurements, the depth to the upper surface of unconsolidated basement is given by

$$d(t) = d_r + 2\kappa T_i \frac{\rho_m}{(\rho_m - \rho_w)} \sqrt{\frac{\kappa t}{\lambda}}, \quad (10.3)$$

where  $d_r$  is the depth to the ridge crest at zero age,  $\alpha$  is the thermal expansivity of the mantle,  $\rho_m$  is the density of the mantle at  $T=T_m$ , and  $\rho_w$  is the density of seawater. The important feature of this model is that the thermal structure, surface heat flow and seafloor depth vary with the square root of age. This model was calibrated by Davis and Lister (1974) using ocean depth data (Sclater, et al., 1971) from the Pacific, Atlantic and Indian oceans (Table 10.1). Half-space cooling models successfully describe seafloor depth for ages younger than 80 Ma (Davis and Lister, 1974).

### 10.2.2. Plate model

The plate model (McKenzie, 1967; Sclater and Franchetau, 1970; Parsons and McKenzie, 1978) differs from half space cooling in that the depth of cooling and the thickness of the thermal boundary layer are limited by a constant temperature lower boundary. This fixed temperature, or sometimes heat flux, is specified at a particular depth, defining the base of the plate. This model was developed to explain the approximately constant heat flow and the cessation of subsidence in old regions.

The mathematical formulation for the plate model is developed in many studies (Parsons and Sclater, 1977; Stein and Stein, 1992; Carlson and Johnson, 1994). We follow the formulation used by Carlson

and Johnson (1994) that makes explicit the exponential age dependence of the geotherm, heat flow, and ocean depth. Temperature as a function of the depth  $z$ , and distance from ridge crest,  $x$ , can be expressed by

$$T(x, z) = T_m \left[ \frac{z}{L} + \sum_n A_n \sin(n\pi x/L) \exp(-\alpha_n z/L) \right] \quad (10.4)$$

where  $T_m$  is the temperature of the plate base,  $L$  is the thermal plate thickness, and

$$A_n = 2/(n\alpha_n), \quad \alpha_n = (Pe^2 + n^2\pi^2)^{1/2} \pi Pe, \quad Pe = vL/(2\kappa). \quad (10.5)$$

$Pe$  is the Peclet number and  $v$  is the plate velocity. Where  $Pe$  is sufficiently large ( $Pe \gg n\pi$ ),  $B_n x/L \sim (n^2\pi^2/L)t$ . With this approximation, Equation (10.4) can be given by

$$T(z, t) = T_m \left[ z/L + \sum_n A_n \sin(n\pi x/L) \exp(-n^2 at) \right] \quad (10.6)$$

for the first few terms of the series when  $n\pi$  is sufficiently small and where  $a = \kappa^2/L^2$ . This formulation makes the exponential dependence on seafloor age explicit. Heat flow as a function of age is given by

$$f(t) = f_m \left[ 1 + 2 \sum_{n=1} \exp(-n^2 at) \right], \quad (10.7)$$

where  $f_m = \kappa T_m/L$  is the asymptotic heat flow for old seafloor. Depth as a function of age is given by

$$d(t) = d_r + d_s \left[ 1 + \sum_j \frac{8}{\pi^2} j^{\pi^2} \exp(-j^2 at) \right] \quad (10.8)$$

where  $j=1,3,5$ ; and  $d_s$  is the asymptotic subsidence of the seafloor given by,

$$d_s = \frac{\sqrt{T_m L \rho_m}}{2(\rho_m \sqrt{\rho_w})} \quad (10.9)$$

Standard reference curves for the plate model were originally given by Parsons and Sclater (1977) and more recently updated by Stein and Stein (1992). Following Stein and Stein (1992), models using parameters given by Parsons and Sclater (1977) and Stein and Stein (1992) are denoted PS77 and GDH1, respectively. PS77 was calibrated using depth data only from the North Pacific and North Atlantic, whereas GDH1 was calibrated using both depth and heat flow (from crust > 50 Ma) from the North Pacific and northwest Atlantic. In order to avoid biasing the age-depth relation and use as much data as possible, both Parsons and Sclater (1977) and Stein and Stein (1992) include data close to hot spots such as Hawaii and Bermuda. GDH1 represents a marked improvement in fit to the expanded data set relative to PS77 (Stein and Stein, 1992). The GDH1 plate is substantially thinner and hotter than PS77 as indicated by the respective model parameters (Table 10.1). Asymptotic values of heat flow are 48 mW m<sup>-2</sup> and 34 mW m<sup>-2</sup>, for GDH1 and PS77, respectively. These values represent the background flow of heat from the asthenosphere carried by convection. The plate models and their predictions characterize the average seafloor, but variations between and within plates are large such that best fitting thermal parameters are different for different ocean basins (Stein and Stein, 1994a). Johnson and Carlson (1992) made a fit of the plate model to DSDP/ODP drilling data (sediment thickness and basement depth) and found best fitting model parameters intermediate between those of PSM and GDH1.

Figure 10.1 shows that for crustal ages younger than 80 to 100 Ma, the depth increases linearly with the square root of age (e.g., Davis and Lister, 1974; Parsons and Sclater, 1977; Sclater and Wixon, 1986; Renkin and Sclater, 1988; Stein and Stein, 1992). Parsons and Sclater (1977) emphasized that because the plate cools from the top down, both the plate model and half space cooling models are essentially the same until cooling has progressed to the point where, in the case of the plate model, further cooling is retarded by the lower boundary condition. The time taken for a thermal disturbance to have a significant effect (16% perturbation) at a given depth is defined by a thermal length calculation where

$$t = \frac{l^2}{4\kappa}. \quad (10.10)$$

For a thermal diffusivity  $\kappa$  of  $8 \times 10^{-7} \text{ m}^2\text{s}^{-1}$ , the thermal length,  $l$ , corresponding to 100 Ma is about 100 km. At ages older than about 100 Ma, ocean depth appears to flatten with respect to the half space model and shows greater variability. One reason for the large variability in bathymetry is that old lithosphere such as the western half of the Pacific plate is densely populated by seamounts and oceanic plateaus (Renkin and Sclater, 1988; Wessel, 2001).

### 10.2.3. A Preferred Reference Model

The choice of an appropriate reference for the thermal evolution of oceanic lithosphere remains somewhat contentious, and depends in part on the objectives at hand. The choice of reference model is not clear-cut because no single model, whether it is a plate model or half space model, adequately explains all of the data (Stein and Stein, 1992; Carlson and Johnson, 1994). Regional variations of ocean depth systematically exceed assigned uncertainties and such departures from the plate model are significant (e.g., Marty and Cazenave, 1989). Overall plate models provide a better fit to heat flow and bathymetric data than half space models, especially for crust of older ages (Figure 10.1). Thus plate models, such as GDH1, provide the best average description of observed heat flow and depth as a function of age and may serve as a reference against which to measure anomalies. The principal drawback of the plate model is that it is a simple mathematical abstraction for a lithosphere consisting of a rigid mechanical and a thermal boundary layer (Parsons and McKenzie, 1978). The plate model does not address the process that limits growth such that the plate thickness and lower boundary temperature are really only parameters of convenience. McNutt (1995) summarizes various candidate processes that might limit the thickness of the lithosphere, but to date these processes remain poorly resolved.

The half space boundary-layer cooling model provides a reasonable fit to cooling for crust as old as 80 – 100 Ma, but predicts deeper ocean depths and lower heat flow values in older lithosphere than are generally observed (Figure 10.1). One possible explanation for the discrepancy involves non uniformitarian processes, whereby major transient thermal events in the past have affected both heat flow and bathymetry for the oldest sea floor. If this is the case, no simple model (i.e., uniform sea floor spreading with constant thermal boundary conditions) could explain all the data (Davis, 1988; Lister et al., 1990). One example of this class of models has been to combine half space cooling with plate reheating (Heestand and Crough, 1981; Carlson and Johnson, 1994; Nagihara et al., 1996). Proponents of the reheating model argue that when the distance from hot spots and hot spot swells is large the seafloor subsides in agreement with the half-space cooling model. The northwest and southwest

Atlantic, two regions relatively unaffected by hotspot activity, subside according to simple half space cooling theory over large areas (e.g., Marty and Cazenave, 1989). Nagihara et al. (1996) pursued this argument by carefully selecting a series of wide flat basins of different crustal ages. In this way topographic subsidence can be used to predict heat flow, with the only model assumption being that the heat flux is related to subsidence through thermal expansivity (Equation 10.3). They found that these basins fall closer to a boundary layer cooling curve than PS77 or GDH1. Furthermore, these basins plot on the age-depth curve younger than their crustal ages, suggesting a reheating event.

For the purpose of having a reference thermal model to evaluate heat deficits in young sea floor and the magnitude of hydrothermal circulation, it seems prudent to select a simple reference model appropriate for young sea floor that satisfies the following criteria: (a) the model should be physically based, (b) when compared with observations, the model should yield anomalies that also have a physical explanation, (c) the model should provide a reasonable fit to available data, and (d) the model should be simple so that observations can easily be compared to model predictions. One should also note that there are many geologic processes that can add or inject heat into the lithosphere such as stretching, plume interaction, intrusion, or magmatic underplating, but few processes extract heat. Thus, most lithospheric thermal anomalies that have a physical explanation (criterion (b)) should be expected to be positive.

A useful analogy can be made to gravity reference models and anomalies. The gravity reference is physically based, being computed for a rotating Earth and given on a reference spheroid by a simple formula. At heights above the reference spheroid one can compute a free air gravity anomaly, a Bouguer gravity anomaly, or an isostatic gravity anomaly, each of which involves different assumptions about mass compensation in the Earth. In each case, gravity anomalies can be explained by mass excesses or deficiencies (caused by rock density distributions) relative to the model assumptions. The fact that the Bouguer gravity prediction fails to match observations at high elevations does not negate the usefulness of the simple and convenient Bouguer gravity anomaly in assessing mass excesses and deficiencies in the crust. Likewise with thermal reference models and thermal anomalies, the failure of the half space model to match observations in sea floor older than 100 Ma does not negate the usefulness of the half-space model in determining heat flow deficits and excesses in much of the sea floor today, and especially in young sea floor.

For assessing the hydrothermal heat flow deficit, we choose as a reference thermal model, particularly applicable in sea floor up to 100 Ma old, the half-space model for which surface heat flow is given by

$$f = \frac{C}{\sqrt{t}}. \quad (10.11)$$

Average seafloor heat flow between ages  $t_1$  and  $t_2$  for the reference model is given by

$$f_{t_1 \square t_2} = \frac{2C}{(t_2 \square t_1)} (\sqrt{t_2} \square \sqrt{t_1}), \quad (10.12)$$

and average heat flow from the mid ocean ridge to an isochron of age  $t$  is

$$q_{avg} = \frac{2C}{\sqrt{t}}. \quad (10.13)$$

A comparison of model predictions with “unperturbed” heat flow data in oceanic crust is shown in Figure 10.2. The data are restricted to well sedimented sites known to be more than 20 km from any basement outcrop to eliminate or minimize the effects of open hydrothermal circulation (Sclater et al., 1976; Davis, 1988). Although the data have considerable variance, especially in sea floor younger than 10 Ma, they show good agreement with an inverse square root age boundary-layer cooling curve out to an age of roughly 100 Ma. A constant value of  $C$  of  $500 \text{ mW m}^{-2} \text{ My}^{1/2}$  provides a good fit to existing data.

For sea floor older than 100 Ma, this reference thermal model consistently predicts heat flow that is lower than observed heat flow by about  $10 \text{ mW m}^{-2}$  just as the Bouguer gravity model prediction is too high by about 200 mGal for large expanses of elevated continents such as western North America. The physical explanation for the Bouguer gravity anomaly is a low density crustal root that is not included in the gravity model. The physical explanation for the old sea floor heat flow anomaly is additional heat into the base of the lithosphere that is not included in the reference model as discussed above.

### 10.3. Hydrothermal Circulation and Heat Flow Deficits

Two common characteristics of heat flow through young seafloor are well illustrated in Figure 10.1. First, while heat flow values are usually higher than the global average, they are substantially lower than predicted by conductive thermal models of lithospheric evolution (the reference model). Second, heat flow values for young crust almost invariably exhibit significantly more variability than observations on older seafloor. Several lines of reasoning suggest both of these observations are due to hydrothermal circulation (Lister, 1972). As discussed previously, the vast majority of heat flow observations are made by inserting a several-meter long heat flow probe into sediments. In areas of hydrothermal circulation, sediment ponds are typically areas of lower than expected heat flow due to the cooling effect of ventilation through surrounding outcrop (Chapters 11 and 12). Heat that would normally reach the surface in the absence of fluid flow is carried laterally to a discharge region. This process lowers the thermal gradient in the overlying sediments over a considerable distance from the outcrops themselves, biasing even randomly distributed heat flow observations towards lower values. This bias is made worse because measurements cannot be made in areas of outcrop where discharge normally occurs. As a result, average heat flow is often well below the reference model prediction, and values significantly greater than the reference level are rarely observed. In areas of significant fluid flow where the sediment-crust interface is nearly isothermal, the thermal gradient will be a strong function of the sediment thickness, accounting for the increased variability in heat flow values. Thermal effects such as chemical reactions between the water and crust that might produce the low observed values are considered negligible (Wolery and Sleep, 1976), and other sources of environmental noise such as sedimentation, recent slumping, and thermal refraction, account for neither the heat flow deficit nor observed variability (e.g. Von Herzen and Uyeda, 1967; Langseth and Von Herzen, 1970).

Figure 10.3 is a multi-scale schematic diagram of such a heat flow deficit representing either an individual survey result, a heat flow compilation for a particular spreading ridge, or a compilation for a global data set. Consider a heat flow deficit  $(f_{\text{obs}} - f_{\text{ref}})$  for an element of sea floor between age  $t_1$  and  $t_2$ . The rate of heat extracted by hydrothermal circulation is

$$F_i = (f_{\text{obs}} - f_{\text{ref}}) A_i \quad (10.14)$$

where  $A_i$  is the area of affected sea floor within the isochrons  $t_1$  and  $t_2$ . The total rate of heat extracted for a particular spreading center or for the global ridge system is the summation of Equation 10.14 for that ridge segment or over all the sea floor exhibiting a heat flow deficit,

$$F_{tot} = \sum F_i \quad (10.15)$$

Sclater et al. (1980; Table A1, and reproduced in modified form by Stein and Stein, 1994b) provide a convenient set of area-age values for the sea floor. The heat extracted from the upper oceanic crust is delivered advectively back into the ocean by a volume flow of water  $Q$  given by

$$Q = \frac{F}{\sum c(T_2 - T_1)} \quad (10.16)$$

where  $c$  is the specific heat of water and  $T_1$  and  $T_2$  are recharge and discharge temperatures respectively at the sea floor (Figure 10.3).

A summary of estimates of global hydrothermal circulation heat loss rates is given in Table 10.2. It is interesting to note that two of these estimates (Williams and Von Herzen, 1974; Wolery and Sleep, 1974) were made before 1979 when the discovery of black smokers provided the first direct evidence of sea floor hydrothermal venting. Williams and Von Herzen (1974) did not perform the summation in Equation 10.15, but instead argued that oceanic heat flow could be partitioned into a background of 47 mW m<sup>-2</sup> and a transient heat flow resulting from lithospheric cooling. Their analysis of heat flow measurements on young crust suggested that only a small part of the transient heat was released by thermal conduction in very young sea floor. They calculated that if all of the transient heat in crust out to 2 Ma (equivalent to half the total transient heat) is removed by hydrothermal circulation, the global advective heat loss rate would be  $8.5 \times 10^{12}$  W, or about 20% of the global heat loss.

Subsequent investigators based their estimates of hydrothermal heat loss on actual integrations of the observed sea floor heat flow deficit. Wolery and Sleep (1974) first performed the integration on a global data set but divided the globe into fast spreading ridges and slow spreading ridges to simplify the integration. Data analyses at that time suggested heat flow deficits to sea floor ages 17 and 23 Ma in fast and slow spreading ridges, respectively, corresponding to a removal of 32 and 42% of lithospheric cooling heat for those ridge systems through hydrothermal convection (Wolery and Sleep, 1974). The

global heat loss rate through advection was computed to be  $5 \times 10^{12}$  W. The global mass flow through the sea floor to account for the advective heat removal was calculated by Wolery and Sleep (1974) to be between  $8.1$  and  $1.3 \times 10^{14}$  kg yr<sup>-1</sup>, assuming discharge temperatures ranging between the limits of 50 and 300 °C respectively.

Sclater et al. (1980) applied the heat flow deficit analysis in a systematic way to all oceans. Using all available data, they computed the average of marine heat flow observations for the five major ocean basins (N. Pacific, S. Pacific, Indian, N. Atlantic, S. Atlantic) for 13 age groups. For each of the age brackets, they compared observed heat flow to a reference heat flow from their lithospheric cooling model (Table 10 of Sclater et al., 1980). The total heat loss rate out to 65 Ma sea floor was computed to be  $10.3 \times 10^{12}$  W with almost 60% of that heat loss occurring in crust younger than 9 Ma. Subsequently, Stein and Stein (1994, 1997) used a global marine heat flow data set filtered for quality (Stein and Abbott, 1991) and averaged into 2 My bins and compared the data to GDH1 to calculate the heat flow deficit as a function of age. Stein and Stein (1994b) estimate a global heat loss rate of  $11 \times 10^{12}$  W. This estimate is larger than previous estimates of hydrothermal heat loss (Table 10.2) for two reasons. GDH1 has a hotter basal reference temperature than used by previous investigators and thus their inferred heat flow deficits are larger for all age brackets. Second, the Stein and Stein (1994) analysis suggests that ventilated hydrothermal circulation extends to crust as old as 65 Ma for all oceans, and thus the integration is performed over a relatively large area of sea floor. The mass flow of  $1.3 \times 10^{15}$  kg/yr inferred from this thermal analysis is also larger than given by previous investigators, but that difference arises primarily from assumptions about discharge temperatures (Equation 10.16). Stein and Stein (1994b) assume that high temperature (250 °C) discharge characterizes sea floor younger than 1 Ma, but that the rest of the sea floor exhibiting a heat flow deficit has a lower temperature discharge of 50 °C. However, even this lower limit may be too high (Wheat and Mottl, Chapter 20).

Elderfield and Schultz (1996) base their off axis advective heat loss estimate on the average heat flow compilation of Stein and Stein (1994b) but used a cooler plate than predicted by GDH1. Elderfield and Schultz (1996) estimate off axis mass flow between  $3.7 - 11 \times 10^{15}$  kg yr<sup>-1</sup> assuming water temperatures in the range of 5 – 15° C.

Two estimates for the cumulative advective heat loss for the globe as a function of sea floor age are shown in Figure 10.4 (Sclater et al., 1980; Stein and Stein, 1994b). Although the temporal extent of this heat loss and the physical conditions that diminish and eventually eliminate the heat flow deficit (e.g., sediment sealing, crustal alteration, and permeability loss) remain uncertain, the result for young sea

floor is robust. About  $5 \times 10^{12}$  W, or half the heat loss rate is associated with sea floor younger than 4 Ma. Two thirds of the advective heat loss occurs in sea floor younger than 8 Ma, and 83 % in crust younger than 20 Ma. Thus the cumulative value of approximately  $10^{13}$  W is unlikely to change significantly by the addition of new data, unless detailed surveys alter our view of the processes that cause heat flow deficits. Although the discharge temperature for ridge flank hydrothermal circulation systems is elusive, the use of temperatures of 50 °C or lower in Equation 10.15 together with the cumulative heat loss yield a global hydrothermal mass flow greater than  $10^{15}$  kg yr<sup>-1</sup>. The mass of the oceans is  $1.37 \times 10^{21}$  kg, so the inferred hydrothermal mass flux suggests that the entire mass of the oceans may cycle through the upper crust in about a million years.

While the global marine heat flow data set yields broad global estimates of hydrothermal heat loss and mass flow (Sclater et al., 1980; Stein and Stein, 1994b, 1995), there are troubling discrepancies between inferences about hydrothermal circulation drawn from the global analyses and those drawn from detailed local studies. For example, the Stein and Stein (1994) analysis of the global data suggests a uniform sealing age of 65 Ma for all oceans. The sealing age is the age at which the observed heat flow merges with the predicted lithospheric heat flow. But several detailed studies, especially on well sedimented ridge flanks, indicate that observed heat flow can equal predicted heat flow at much younger ages: 7-8 Ma at the Galapagos Spreading Center (Sclater et al., 1974), 5-6 Ma for the Costa Rica rift (Langseth et al., 1983), and 1.5 Ma for the eastern flank of the Juan de Fuca Ridge (Davis et al., 1999). And in other enigmatic settings, heat flow deficits have been found to be unusually large, such as in the region of generally well sedimented seafloor off central America (Langseth and Silver, 1996; Fisher et al., in press). Also the global analysis (Stein and Stein, 1994b) concluded that sediment thickness plays a relatively minor role governing the longevity of hydrothermal circulation, whereas numerous local studies have pointed to the importance of sediment thickness, completeness of sediment cover, and basement relief as having controlling local influences on the vigor, pattern, and degree of ventilation of hydrothermal circulation ( Sclater et al., 1970, 1974, 1976; Lister, 1972; Anderson and Hobart, 1976; Davis and Lister, 1977; Anderson et al., 1977; Davis et al., 1989, 1999; Abbott et al., 1992; Chapter 6). These discrepancies may result from the vintage of heat flow measurements and increasing recognition that environmental factors provide a strong control on the nature of heat transfer. Many measurements in the global heat flow data set are often 50 to 100 km apart and have only sparse environmental information (basement relief, sediment thickness and cover extent). In contrast modern surveys have paid more attention to environmental controls with complementing seismic surveys and extensive swath

mapping. With greater ability to navigate precisely and dynamically hold the ships position (often to within meters) heat flow transects with penetrations only 10's to 100's of meters apart are becoming more routine. These closely spaced measurements coupled with environmental information are revealing new insights into the nature of hydrothermal circulation. Nevertheless, much has been learned from the global heat flow data set.

Hydrothermal circulation undoubtedly evolves with the aging of oceanic crust (Figure 10.5) (Lister, 1972, 1983; Davis and Lister, 1977; Jacobson, 1992; Stein and Stein, 1994b; Carlson, 1998). In young sea floor near ridge axes, hydrothermal circulation is characterized by rapid flow rates, and unencumbered exchange of sea water with the crystalline crust. This style of circulation is manifested in heat flow values that are significantly lower than predicted by cooling models of oceanic lithosphere. Heat flow values of 10 to 20% of the reference heat flow are not uncommon, and heat flow is highly variable (Figure 10.5). The convective regime is not radically changed with the gradual addition of sediment, especially if the sediment cover is incomplete and concentrated to sediment ponds within an otherwise bare rock environment. Because measurements can be made in basement lows where sediment is available, this environment is strongly represented in heat flow compilations. Standard deviations of heat flow surveys in this regime can be  $70 \text{ mWm}^{-2}$  or more, with total variability even greater, i.e., comparable to the mean measured heat flow (e.g. Sclater et al., 1974). With greater age and the addition of more hydraulically resistive sediment, the hydrothermal circulation evolves from open to closed circulation (Figure 10.5), but until the sediment is sufficiently thick and continuous to isolate the permeable igneous crust from the ocean, there may still be significant leakage through infrequent basement ridges and partially buried seamounts. Such leakage may produce very high but geographically concentrated heat flow anomalies surrounded by broad areas with as much as 50% heat flow deficit. Variability in heat flow over rough basement topography with complete sediment drape can still be high (Figure 10.5), but once the sediment has effectively isolated circulation within the igneous crust from exchange with the ocean, the mean heat flow values approach the reference value. Closed circulation redistributes heat within the circulation system but the integrated surface heat flow must be equal to the cooling lithospheric heat flow in this regime. Given that basement topography exerts a significant control on the heat flow pattern, incomplete spatial sampling can still produce a bias towards lower heat flow. Finally, even in moderately young sea floor where hydrothermal circulation exists, heat flow in regions of thick, extensive sediment cover and smooth sea floor is close to that expected from cooling lithosphere models and the variability is reduced to about  $20 \text{ mW m}^{-2}$ , a level

close to the uncertainties imposed by inherent observational errors. Evidence for closed circulation on old oceanic crust (> 60 m.y.) is covered in detail by Von Herzen (Chapter 13).

Drawing conclusions from the global heat flow data set (at the local scale) is a problem in multivariate analysis where many of the important variables describing the local environment are often poorly known. At the local scale, inferences drawn from the global heat flow data set may not be particularly helpful. In contrast local surveys with dense data coverage provide greater context for interpreting heat flow deficits in young oceanic crust. One such example is considered next.

#### **10.4. The Eastern Flank of the Juan de Fuca Ridge**

The eastern flank of the northern Juan de Fuca Ridge has been the setting for numerous studies of heat flow and hydrothermal circulation in young oceanic crust. There is extensive sediment cover on sea floor as young as 0.6 Ma, a variety of basement environments (flat areas, basement ridges, and isolated outcrops referred to as permeable penetrators), and relatively easy access. With respect to sedimentation, the eastern flank of the Juan de Fuca ridge is anomalous. However, these sediments allow the relatively high density of heat flow measurements to be made and shows conclusively that sediment exerts a strong influence on the age at which the heat flow deficit becomes negligible (Davis et al., 1999).

The main heat flow result from this area is shown in Figure 10.6. Heat flow is shown for a transect that starts about 20 km from the ridge axis where sea floor age is 0.6 Ma and continues to the southeast for about 100 km where the sea floor age is 3.7 Ma. Heat flow nearest the axial region of igneous rock outcrop is only  $100 \text{ mW m}^{-2}$ , about 15 % of that expected from cooling lithosphere models, but increases to expected heat flow over a distance of about 20 km where the age of the sea floor is 1.2 Ma. Heat flow along the entire transect is very coherent; the local variability at the kilometer scale is closely related to buried basement topography, with high heat flow over topographic highs and low heat flow over topographic lows. The systematic increase in heat flow away from the basement outcrop can be explained by lateral flow of cool seawater from the area of extensive outcrop in the vicinity of the ridge axis into the upper igneous crust that lies under the sediment cover. The rate of flow is estimated to be of the order of meters to tens of meters per year (Davis et al., 1999; Stein and Fisher, 2002; Chapter 11), although the details of flow, including recharge, discharge, and local convective mixing, cannot be determined.

The observation that heat flow returns to the reference value predicted from lithosphere cooling at 1.2 Ma does not mean that hydrothermal circulation ceases at that point. Quite to the contrary, there is considerable evidence to suggest the presence of vigorous closed convection within the igneous crust throughout the transect. Downward continuation of heat flow values along the transect in Figure 10.6 (Davis et al., 1989) initially suggested that the top of the basement beyond 1.5 Ma crust was roughly isothermal at a temperature between 50 and 70°C. This inference has subsequently been confirmed by drilling and post drilling observations along the ODP Leg 168 transect (Davis et al., 1997) where temperatures determined at the top of the basement for a considerable part of the transect varied only from 60-64°C in spite of considerable variations in depth to basement (Figure 10.6). The most convincing confirmation of the isothermal uppermost basement temperature condition comes from ODP Sites 1026 and 1027 (separated by 2.2 km). Whereas sediment thickness differs by a factor of 2.5, the basement temperatures differ by only 2°C. Such an isothermal condition requires vigorous convection (Chapters 8 and 12).

The conditions that exist on the Juan de Fuca Ridge also provide an opportunity for interpolating heat flow between measurement points and estimating continuous profiles or maps of heat flow across the sea floor. Such profiles and maps allow true spatial integration of heat flow and heat flow deficits. A continuous heat flow profile for the Juan de Fuca Ridge (Figure 10.6) was made by combining seafloor heat flow data, sediment physical and thermal properties, seismic reflection times to basement, and ODP measurements of basement depth and temperature (Davis et al., 1999). The continuous profile shows a heat flow deficit in crust younger than 1.2 Ma but the mean heat flow for sea floor older than 1.2 Ma agrees remarkably well with half space cooling when averaged over a spatial scale that fully spans the scale of local variability (Figure 10.6).

The heat flow deficit over the sedimented sea floor between ages 0.6 and 1.2 Ma (Figure 10.6c) has been integrated to yield a cumulative heat loss of about 3 MW/ km of strike length for this section of the Juan de Fuca Ridge (Davis et al., 1999). If the conductive heat flow over the bare-rock section from 0-0.6 Ma sea floor is no more than the 100 mW m<sup>-2</sup> observed at the sediment onlap, then an additional 16 MW/km strike length is being lost by advection over bare rock for a total heat loss rate of 19 MW/km strike length. Thus a value of about 20 MW/ km-strike-length is a robust minimum for mid ocean ridge advective heat loss; advective heat loss on ridges with less sediment and therefore a greater area to host open-exchange circulation (Figure 10.5) could be as high as 170 MW/km-strike-length if open exchange continues to a more typical sea floor age of 65 Ma as suggested by Stein and Stein (1994b).

The advantage of detailed heat flow studies over global statistical studies in understanding hydrothermal processes in the sea floor is highlighted in Figure 10.6, by compressing all the 0-2 Ma heat flow data for the transect into a single bin as would be done in the global compilations. The average of 96 measurements is  $389 \text{ mW m}^{-2}$  with a standard deviation of  $131 \text{ mW m}^{-2}$ . Although this single value would be interpreted to have a deficit of  $318 \text{ mW m}^{-2}$  compared to the average expected heat flow of  $707 \text{ mW m}^{-2}$  for sea floor 0-2 Ma, neither the return to predicted heat flow at 1.2 Ma, the important correlation of heat flow with basement topography, nor the nature of the heat flow deficit recovery would have been revealed.

### 10.5. Discussion

Recent, high density heat flow surveys collocated with extensive seismic profiling and often accompanied by piston coring, pore water chemistry, and ODP drilling are shedding new light on controls for hydrothermal convection in young sea floor (Davis et al., 1989, 1999; Grevenmeyer et al., 1999; Harris et al., 2000; Fisher et al., in press). Not only do these detailed studies give guidance on how marine heat flow surveys focused on hydrothermal convection should be conducted in the future, but they also provide insight for interpreting the large body of data gathered under less ideal conditions, limited instrumentation, and imprecise navigation. Most critically, the detailed surveys confirm how important it is to understand the environment surrounding the heat flow sites; this includes defining sediment thickness variations, extent of sediment cover, and basement relief.

It appears that the heat flow deficit (the locally averaged observed heat flow relative to that expected from lithosphere cooling models; Figure 10.5) remains a robust measure of the ventilation efficiency of open, hydrothermal convection beneath the sea floor. Heat is extracted by pore water circulation systems recharging and discharging in bare-rock environments where heat flow probe measurements are precluded.

The spatially integrated heat flow deficit over the area of the sea floor hosting ventilated convection provides an estimate of the advective heat loss rate for a particular spreading ridge. Older data compilations are useful for such calculations, although more recent studies with close station spacing and/or a continuous heat flow profile inferred from determinations of basement temperature and burial depth provide a more precise estimate of local heat loss. The most uncertain parameter in converting advective heat loss into mass flow through the upper oceanic crust is basement fluid temperature.

Current global estimates of mass flow computed from heat loss observations vary from  $10^{15}$  to  $10^{14}$  kg/yr (Table 10.2), corresponding to the entire ocean mass passing through the upper oceanic crust every 1 to 10 My respectively.

There is likely a transition in the heat flow patterns between sea floor that has ventilated convection and sea floor with sufficient thickness and areal extent of sediment to prevent significant thermally significant recharge of sea water into the permeable igneous crust and discharge of hydrothermal water back to the ocean. In transition regions, the average measured heat flow must increase from a fraction to the full expected heat flow value, and variability may fall (Figure 10.5). In the absence of spatial biasing (e.g., where measurements are preferentially made in low heat flow environments) the integrated or average heat flow over closed convection systems should equal the lithospheric reference heat flow. High variability in heat flow can persist in spite of thick sediments, however, if there is considerable basement relief, especially if there is vigorous, closed hydrothermal circulation in the upper igneous crust.

A useful test for hydrothermal circulation in a sedimented environment of the sea floor would be a “topo test” in which a closely spaced heat flow survey would be conducted over seismically imaged rough basement topography (Figure 10.7). A “topo test” in marine heat flow would be analogous to the fold test in paleomagnetism. In the fold test, remanent magnetizations are determined at multiple positions in a single bed (isochron) following the fold. If the remanent magnetizations are unidirectional in the folded geometry, it is inferred that the magnetization was acquired post folding. If the magnetization exhibited the rotations of the fold, and unfolding the bed restores a unidirectional remanent magnetization, then it can safely be assumed that magnetization was acquired prior to folding.

Figure 10.7 illustrates the diagnostic feature of a topo test for hydrothermal circulation. If convection is sufficiently vigorous to create a near-isothermal condition at the top of the permeable igneous basement, then this state will be manifested by heat flow that is inversely proportional to sediment thickness (Figure 10.7a). High heat flow will occur over buried topographic ridges and seamounts and low heat flow will occur over thickly buried topographic troughs. If hydrothermal circulation does not exist, or if it is insufficiently vigorous to thermally homogenize the upper crust (see Figure 8.2), the heat flow across rough topography will be constant except for a relatively small thermal refraction and sedimentation effect (Chapter 13). A plot of heat flow versus sediment thickness (Figure 10.7d) illustrates how large the difference can be between convective and conductive regimes in the topo test. This plot shows data gathered over a basement ridge-trough configuration on the Juan de Fuca

ridge flank (Figure 10.7c) (Davis et al., 1989) and confirms the existence of hydrothermal circulation (Figure 10.7d).

In the absence of detailed knowledge about the environment of the heat flow sites, as is the case for much of the older data, one can still exploit the variability of the heat flow results to make inferences about convection (Chapter 13). Both heat flow variability and the variability normalized by measured heat flow in age groups decrease with age of sea floor (Stein and Stein, 1994b). The decline in variability is inferred to reflect a decline in hydrothermal activity. It may also be a simple consequence of greater sediment thickness, however; detailed studies are required to resolve this ambiguity.

Where extensive marine heat flow surveys have been completed, they have provided a rich data set for examining the process of hydrothermal circulation in the oceanic crust. A continuing goal of marine heat flow studies should be to document for many ridge systems the nature and extent of the three basic thermal regimes: the open circulation regime whose heat flow deficit leads to estimates of heat loss rates and mass fluxes of sea water through the oceanic crust; the closed circulation convection regime where exchange of sea water with the convection cells is precluded by hydraulically resistive sediments; and the purely conductive regime where reduced permeability of the crust and reduced driving forces in older and cooler lithosphere combine to shut down convection.

## 10.6. Conclusions and Recommendations

1. Heat flow remains one of the most useful observational constraints when studying cooling models for oceanic lithosphere and hydrothermal circulation within oceanic crust.
2. For seafloor younger than about 100 Ma, a convenient and useful reference curve for lithospheric cooling is  $C/\sqrt{Age}$ . This reference curve is simple, physically based on boundary-layer cooling theory, and yields anomalies that are also physically based. A value of  $C=500 \text{ mW m}^{-2} \text{ My}^{1/2}$  provides a good fit to reliable data. For lithosphere older than 80 – 100 Ma, heat flow levels out at about  $45\text{-}50 \text{ mW m}^{-2}$  as a consequence of some form of chronic or episodic heating from great depth.
3. Global analyses of heat flow data grouped into regular age bins for oceanic crust have been historically important in leading to the recognition of hydrothermal convection as a mechanism to

explain heat flow deficits in young sea floor. Global analyses yield average results on global heat flow deficits, and heat loss rates.

4. Heat loss rates for the entire oceanic ridge system is about  $10^{13}$  W with about 2/3 of the heat loss occurring in sea floor younger than 8 Ma. The mass flow necessary to produce this heat loss is about  $10^{15}$  kg/yr equivalent to fluxing the entire mass of the oceans through the upper crust every million years. However, the total mass flow depends on the temperature drop which is not well defined, thus this mass flow estimate is approximate.

5. Improved estimates for total mass flow required an improved understanding of processes controlling hydrothermal circulation, and this will depend on new closely spaced heat flow surveys with particular attention paid to the environment in which the thermal measurements are being made. In particular, constraints on sediment thickness are required to determine basement fluid temperatures.

6. Although carried out in an atypical seafloor environment (high sedimentation rate), experiments on the eastern flank of the Juan de Fuca ridge provide a useful template for studying thermal aspects of hydrothermal circulation on the sea floor. The combination of closely spaced heat flow determinations with collocated seismic profiling and strategic cores for sampling pore fluids offers the greatest opportunity for understanding hydrothermal circulation.

#### Acknowledgments

This paper benefited from useful discussions with C. Stein, A. Fisher and reviews by R. Von Herzen, and C. Jaupart. US National Science Foundation grant OCE-0001944 supported this work.

## References

- Abbott, D. H., C. A. Stein, and O. Diachok, 1992, Topographic relief and sediment thickness: their effects on the thermal evolution of the oceanic crust, *Geophys. Res. Lett.*, 19: 1975-1978.
- Anderson, R. N., and M. A. Hobart, 1976, The relation between heat flow, sediment thickness, and age in the eastern Pacific, *J. Geophys. Res.*, 81: 2968-2989.
- Anderson, R. N., M. G. Langseth, and J.G. Sclater, 1977. The mechanisms of heat transfer through the floor of the Indian Ocean. *J. Geophys. Res.*, 82:3391-3409.
- Becker, K., and R. P. Von Herzen, 1983. Heat transfer through the sediments of the Mounds Hydrothermal area, Galapagos Spreading Center at 86°W. *J. Geophys. Res.*, 88:995-1008.
- Carlson, R. L., 1998, Seismic velocities in the uppermost oceanic crust: age dependence and the fate of layer 2A, *J. Geophys. Res.*, 103: 7069-7077.
- Carlson, R. L., and H. P. Johnson, 1994, On modeling the thermal evolution of the oceanic upper mantle: an assessment of the cooling plate model, *J. Geophys. Res.*, 99: 3201-3214.
- Chapman, D. S., and H. N. Pollack, 1975, Global heat flow: a new look, *Earth Planet. Sci. Lett.*, 28, 23-32.
- Davis, E. E., 1988, Thermal aging of oceanic lithosphere, in *Handbook of Seafloor Heat Flow*, ed. by J. A. Wright and K. E. Loudon, CRC Press, 145-168.
- Davis, E. E., D. S. Chapman, C. B. Forster, and H. Villinger, 1989. Heat-flow variations correlated with buried basement topography on the Juan de Fuca ridge flank. *Nature*, 342, 533-537.
- Davis, E. E., D. S. Chapman, H. Villinger, S. Robinson, J. Grigel, A. Rosenberger, and D. Pribnow, 1997, Seafloor heat flow on the eastern flank of the Juan de Fuca Ridge: data from "Flankflux" studies through 1995, eds. Davis, E.E., A.T. Fisher, J.V. Firth, et al., *Proc. ODP Init Repts*, 168, pp. 23-33, College Station, TX.
- Davis, E. E., D. S. Chapman, K. Wang, H. Villinger, A. T. Fisher, S. W. Robinson, J. Grigel, D. Pribnow, J. Stein, and K. Becker, 1999, Regional heat-flow variations across the sedimented Juan de Fuca Ridge eastern flank: constraints on lithospheric cooling and lateral hydrothermal heat transport, *J. Geophys. Res.*, 104: 17,675-17,688.
- Davis E. E., and C. R. B. Lister, 1974, Fundamentals of ridge crest topography, *Earth Planet.*

- Sci. Lett.*, 21: 405-413.
- Davis, E. E., and C. R. B. Lister, 1977, Heat flow measured over the Juan de Fuca Ridge: Evidence for widespread hydrothermal circulation in a highly heat transportive crust, *J. Geophys. Res.*, 82: 4845-4860.
- Elderfield, H., and A. Schultz, 1996, Mid-ocean ridge hydrothermal fluxes and the chemical composition of the ocean, *Ann. Rev. Earth Planet. Sci.*, 24, 191-224.
- Fisher, A. T., and K. Becker, 1995. Correlation between seafloor heat flow and basement relief: observational and numerical examples and implications for upper crustal permeability. *J. Geophys. Res.*, 100:12641-12657.
- Fisher, A. T., K. Becker, and T. N. Narasimhan, 1994, Off-axis hydrothermal circulation: parametric tests of a refined model of processes at Deep Sea Drilling Project/Ocean Drilling Program site 504, *J. Geophys. Res.*, 99: 3097-3121.
- Fisher, A.T., C.A. Stein, R.N. Harris, K. Wang, E.A. Silver, M. Hutnak, A. Cherkaoui, and R. Bodzin, in press, Abrupt transitions in seafloor heat flow reveal hydrothermal boundary near plate suture, *Geophys. Res. Lett.*
- Fowler, C. M. R., 1990, *The Solid Earth*, 472 pp., Cambridge Univ. Press, Cambridge, UK.
- Grevemeyer, I., N. Kaul, H. Villinger, and W. Weigel, 1999, Hydrothermal activity and the evolution of the seismic properties of upper oceanic crust, *J. Geophys. Res.*, 104: 5069-5079.
- Harris, R. N., R. P. Von Herzen, M. K. McNutt, G. Garven, and K. Jordahl, 2000, Submarine hydrogeology of the Hawaiian archipelagic apron 1. Heat flow patterns north of Oahu and Maro Reef, *J. Geophys. Res.*, 105: 21,353-21,369.
- Heestand, R. L., and S. T. Crough, 1981, The effect of hot spots on the oceanic age-depth relation, *J. Geophys. Res.*, 86, 6107-6114.
- Jacobson, R. S., Impact of crustal evolution on changes of the seismic properties of the uppermost oceanic crust, *Rev. Geophys.*, 30: 23-42.
- Jessop, A. M., M. Hobart, and J. G. Sclater, *World Wide Compilation of Heat Flow Data, Geothermal Ser.*, no. 5, Department of Energy, Mines and Resources, Ont.
- Johnson, H. P., and R. L. Carlson, 1992, Variation of sea floor depth with age: a test of models based on drilling results, *Geophys. Res., Lett.*, 19: 1971-1974.
- Johnson, H. P., and M. Hutnak, 1996, Conductive heat flow measured in unsedimented regions of the seafloor, *Eos, Trans., AGU*, 77, 321,324.

- Langseth, M.G., and R. P. Von Herzen, 1970, Heat flow through the floor of the world oceans, in *The Sea*, vol. 4, part 1, edited by A.E. Maxwell, pp. 299-352, Wiley Interscience, New York.
- Langseth, M. G., J. R. Cann, J. H. Natland, and M. Hobart, 1983. Geothermal phenomena at the Costa Rica Rift: Background and objectives for drilling at Deep Sea Drilling Project Sites 501, 504, and 505. In Cann, J.R., Langseth, M.G., Honnorez, J., *et al.*, *Init. Repts. DSDP*, 69: Washington (U.S. Govt. Printing Office), 5-29.
- Lee, W. H. K., and S. Uyeda, 1965, Review of heat flow data, in *Terrestrial Heat Flow, Geophys. Monogr.*, vol. 8, ed. by W.H.K. Lee, pp. 87-190, AGU, Washington, D.C.
- Lister, C. R. B., 1972, On the thermal balance of a mid-ocean ridge, *Geophys. J. Int.*, 26: 515-535.
- Lister, C. R. B., 1983, The basic physics of water penetration into hot rocks, in *Hydrothermal Processes at Seafloor Spreading Centers*, edited by P.A. Rona, K. Bostrom, L. Laubier, and K.L. Smith Jr., pp. 141-168, Plenum, New York.
- Lister, C. R. B., J. G. Sclater, E. E. Davis, H. Villinger, and S. Nagihara, 1990, Heat flow maintained in ocean basins of great age: Investigations in the north-equatorial west Pacific, *Geophys. J. Int.*, 102: 603-630.
- Marty J. C., and A. Cazenave, 1989, Regional variations in subsidence rate of oceanic plates: a global analysis, *Earth Planet. Sci. Lett.*, 94: 301-315.
- McKenzie, D. P. 1967, Some remarks on heat flow and gravity anomalies, *J. Geophys. Res.*, 72: 6261-6273,
- McNutt, M. K., 1995, Marine geodynamics: depth-age revisited, *Rev. Geophys.*, Supp. 413-418.
- Nagihara, S., C. R. B. Lister, and J. G. Sclater, 1996, Reheating of old oceanic lithosphere: deductions from observations, *Earth Planet. Sci. Lett.*, 139: 91-104.
- Parker, R. L. and D. W. Oldenburg, 1973, Thermal model of ocean ridges, *Nature Phys. Sci.*, 242: 137-139.
- Parsons, B., and J. G. Sclater, 1977, An analysis of the variation of ocean floor bathymetry and heat flow with age, *J. Geophys. Res.*, 82: 803-827.
- Pollack, H. N., S. J. Hurter, and J. R. Johnston, 1993, Heat flow from the Earth's interior: analysis of the global data set, *Rev. Geophys.*, 31, 267-280.
- Renkin, M. L., and J. G. Sclater, 1988, Depth and age in the North Pacific, *J. Geophys. Res.*, 93: 2919-2935.

- Sclater, J. G., R. N. Anderson, and M. L. Bell, 1971, Elevation of ridges and evolution of the central eastern Pacific, *J Geophys. Res.*, 76: 7888-7915.
- Sclater, J. G., and J. Crowe, 1979, A heat flow survey at anomaly 13 on the Reykjanes ridge: a critical test of the relation between heat flow and age, *J. Geophys. Res.*, 84, 1593-
- Sclater, J. G., J. Crowe, and R. N. Anderson, 1976. On the reliability of ocean heat flow averages. *J. Geophys. Res.*, 81:2997-3006.
- Sclater, J. G., and J. Francheteau, 1970, The implications of terrestrial heat flow observations on current tectonic and geochemical models of the crust and upper mantle, *Geophys. J. R. Astr. Soc.*, 20: 509-542.
- Sclater, J. G., Jaupart, C., and Galson, D., 1980. The heat flow through oceanic and continental crust and the heat loss of the Earth. *Rev. Geophys. Space Phys.*, 18:269-311.
- Sclater, J. G., R. P. Von Herzen, D. L. Williams, R. N. Anderson, and K. Klitgord, 1974, The Galapagos spreading centre: heat-flow in the north flank, *Geophys. J. R. Astron. Soc.*, 38: 609-626.
- Sclater J. G., and L. Wixon, 1986, The relationship between depth and age and heat flow and age in the western North Atlantic. In *The Western North Atlantic Region*, edited by P. R. Vogt and B. E. Tucholke, pp. 257-270, Geol. Soc. Am., Boulder, Colo.
- Sleep N. H., and T.J. Wolery, 1978, Egress of hot water from the midocean ridge hydrothermal systems: some thermal constraints, *J. Geophys. Res.*, 93: 5913-5922.
- Stein, J. S., and A. T. Fisher, 2002, Multiple scales of hydrothermal circulation in Middle Valley, northern Juan de Fuca Ridge: physical constraints and geologic models, *J. Geophys. Res.*, 106, 8563-8580.
- Stein, J. S., and A. T. Fisher, Observations and models of lateral hydrothermal circulation on a young ridge flank: reconciling thermal, numerical and chemical constraints, *Geochem., Geophys., Geosystems*, in review, 2003.
- Stein, C. A., and S. Stein, 1992, A model for the global variation in oceanic depth and heat flow with lithospheric age, *Nature*, 359: 123-129.
- Stein C.A., and S. Stein, 1994a, Comparison of plate and asthenospheric flow models for the thermal evolution of oceanic lithosphere, *Geophys. Res. Lett.*, 21: 709-712.
- Stein, C.A., and S. Stein, 1994b, Constraints on hydrothermal heat flux through the oceanic lithosphere from global heat flow, *J. Geophys. Res.*, 99: 3081-3095.

- Stein C. A., S. Stein, and A. M. Pelayo, 1995, Heat flow and hydrothermal circulation, In *Seafloor hydrothermal systems*, ed. S.E. Humphris, R.A. Zierenberg, L.S. Mullineaux, and R.E. Thompson, pp. 425-455, Geophys. Mon. 91, Washington, D.C.
- Stein, S., and C. A. Stein, 1997, Sea-floor depth and the Lake Wobegon effect, *Science*, 275: 1613-1614.
- Turcotte D. L. and E. R. Oxburg, 1967, Finite amplitude convective cells and continental drift, *J. Fluid Mech.*, 28: 29-42.
- Turcotte, D. L., and G. Schubert, 1982, *Geodynamics: applications of continuum physics to geologic problems*, 450 pp., Wiley and Sons, New York.
- Von Herzen, R. P., and S. Uyeda, 1967, Heat flow through the eastern Pacific ocean floor, *J. Geophys. Res.*, 68: 4219-4250.
- Wessel, P., 2001, Global distribution of seamounts inferred from gridded Geosat/ERS-1 altimetry, *J. Geophys. Res.*, 106: 19,431-19,441.
- Williams, D. L., and R. P. Von Herzen, 1974. Heat loss from the Earth: new estimate. *Geology*, 2:327-330.
- Williams, D. L., R. P. Von Herzen, J. G. Sclater, and R. N. Anderson, 1974. The Galapagos spreading centre: lithospheric cooling and hydrothermal circulation. *Geophys. J. R. Astron. Soc.*, 38:587-608.
- Wolery T. J., and N. H. Sleep, 1976, Hydrothermal circulation and geochemical flux at mid-ocean ridges, *J. Geol.*, 84: 249-275.

Table 10.1. Model Parameters

Model		Half Space	Plate Cooling Models	
		Cooling	HS74 <sup>a</sup>	PS77 <sup>b</sup>
Initial Temperature (°C)	$T_i$	1120 - 1220	--	--
Thermal Diffusivity ( $\text{m}^2 \text{s}^{-1}$ )	$\kappa$	$8 \times 10^{-7}$	$8 \times 10^{-7}$	$8 \times 10^{-7}$
Thermal Conductivity ( $\text{W m}^{-1} \text{K}^{-1}$ )	$\lambda$	3.3	3.1	3.1
Thermal Expansivity ( $\text{K}^{-1}$ )	$\alpha$	$4 \times 10^{-5}$	$3.28 \pm 1.19 \times 10^{-5}$	$3.1 \pm 0.8 \times 10^{-5}$
Mantle Density ( $\text{kg m}^{-3}$ )	$\rho_m$	3300	3330	3300
Water Density ( $\text{kg m}^{-3}$ )	$\rho_w$	1000	1000	1000
Plate thickness (km)	a	--	$125 \pm 10$	$95 \pm 15$
Basal Temperature (°C)	$T_m$	--	$1333 \pm 274$	$1450 \pm 250$
Ridge Depth (m)	$d_r$	2500	2500	2600

<sup>a</sup>HS74 (Davis and Lister, 1974)

<sup>b</sup>PS77 (Parsons and Sclater, 1977)

<sup>c</sup>GDH1 (Stein and Stein, 1992)

Table 10.2. Estimates of Heat Flow Deficit based on Thermal Measurements

Study	Age Range	Advective Heat Loss	Fluid Circulation Temperatur e	Mass Flow
	Ma	W	°C	kg yr <sup>-1</sup>
Williams and Von Herzen (1974)	0 - 2	$8.5 \times 10^{12}$		--
Wolery and Sleep (1976)	0 - 17	$5 \times 10^{12}$	50 - 300	$1.3 - 8.1 \times 10^{14}$
Sclater et al. (1980)	0 - 50	$10 \times 10^{12}$		--
Stein and Stein (1994b)	1 - 65	$11 \times 10^{12}$	~50	$1.3 \times 10^{15}$
Elderfield and Schultz (1996)	1 - 65	$7 \times 10^{12}$	5-15	$3.7 - 11.0 \times 10^{15}$

## Figure captions

Figure 10.1. Depth of the sea floor (a and b) and heat flow (c and d) as functions of sea floor age. Data come from the analysis of Stein and Stein (1992); they are sorted into 2 My age bins and plotted as bin average (solid circles) and standard deviation (brackets). Curves show model predictions for a half space lithosphere cooling model (solid curve), a plate model (long dashes) and a modified plate model GDH1 (short dashes) See Table 10.1. for model parameters.

Figure 10.2. Reliable heat flow data for young sea floor (Sclater et al., 1976) plotted against the reciprocal square root of age (in Ma) to test model predictions. Solid lines represent half space lithosphere cooling models for values of the constant  $C$  (Equation 10.11) equal to 475, 500, and 525  $\text{mW m}^{-2} \text{My}^{1/2}$  respectively. Modified from Davis (1988).

Figure 10.3. Schematic diagram illustrating a heat flow deficit resulting from open hydrothermal circulation in the oceanic crust. A deficit (shaded region) exists when the heat flow measurements (solid circles) are systematically lower than a reference curve (solid line) for modeled lithosphere cooling. Deficits exist because most heat flow measurements are made in sediment ponds where fluid recharge in surrounding outcrop carries away some of the lithospheric heat flow. Note that for significant advective heat loss, rapid recharge also needs to take place in areas of where basement crops out. The integrated heat flow deficit gives an estimate of the heat lost through the sea floor by advection  $Q$  and mass flux of water  $F$  needed to extract that heat.

Figure 10.4. Cumulative heat loss rate for all oceans resulting from hydrothermal convection. Curves were estimated by integrating the heat flow deficit (defined using the preferred lithospheric reference of Section 10.2.3) between sea floor isochrons over the area of the sea floor between the same isochrons.

Figure 10.5. Cartoon showing possible hydrothermal convection patterns and their heat flow consequences for six hydrologic environments with varying basement relief and sediment cover. Crustal age generally increases to the right.

Figure 10.6. Heat flux, basement temperature, and seismic section for a Juan de Fuca ridge flank transect crossing through ODP Leg 168 drilling Sites 1023-1032. (a) Heat flow measured at the seafloor (dots) and estimated on the basis of sediment thickness and basement temperatures (line). (b) Basement temperatures measured at drilling sites (dots) and interpolated between drilling sites (line). (c) Seismic travel time to the seafloor and basement (from Davis et al., 1999), and locations of Leg 168 drilling sites. Modified from Davis et al. (1999).

Figure 10.7. Topographic test for hydrothermal circulation. a) Schematic diagram showing heat flow patterns over basement relief with vigorous convection. b) Schematic diagram showing heat flow pattern over basement relief with no convection. Variations due to the contrast in thermal conductivity between the basement and overlying sediments are normally small. c) An example, from the eastern flank of the Juan de Fuca Ridge, of heat flow over basement relief with vigorous convection. In this example the basement sediment interface is approximately isothermal. Solid circles indicate raw heat flow determinations, open circles denote heat flow corrected for the thermal effects of sedimentation. Dashed line shows the theoretical heat flow expected for the age of seafloor. Basement temperatures are estimated based on uncorrected heat flow and the sediment thickness as determined from the seismic reflection profile (Davis et al., 1989). d) Observed heat flow as a function of sediment thickness for all values in the study area (Davis et al., 1989). Modified from Davis et al. (1989).

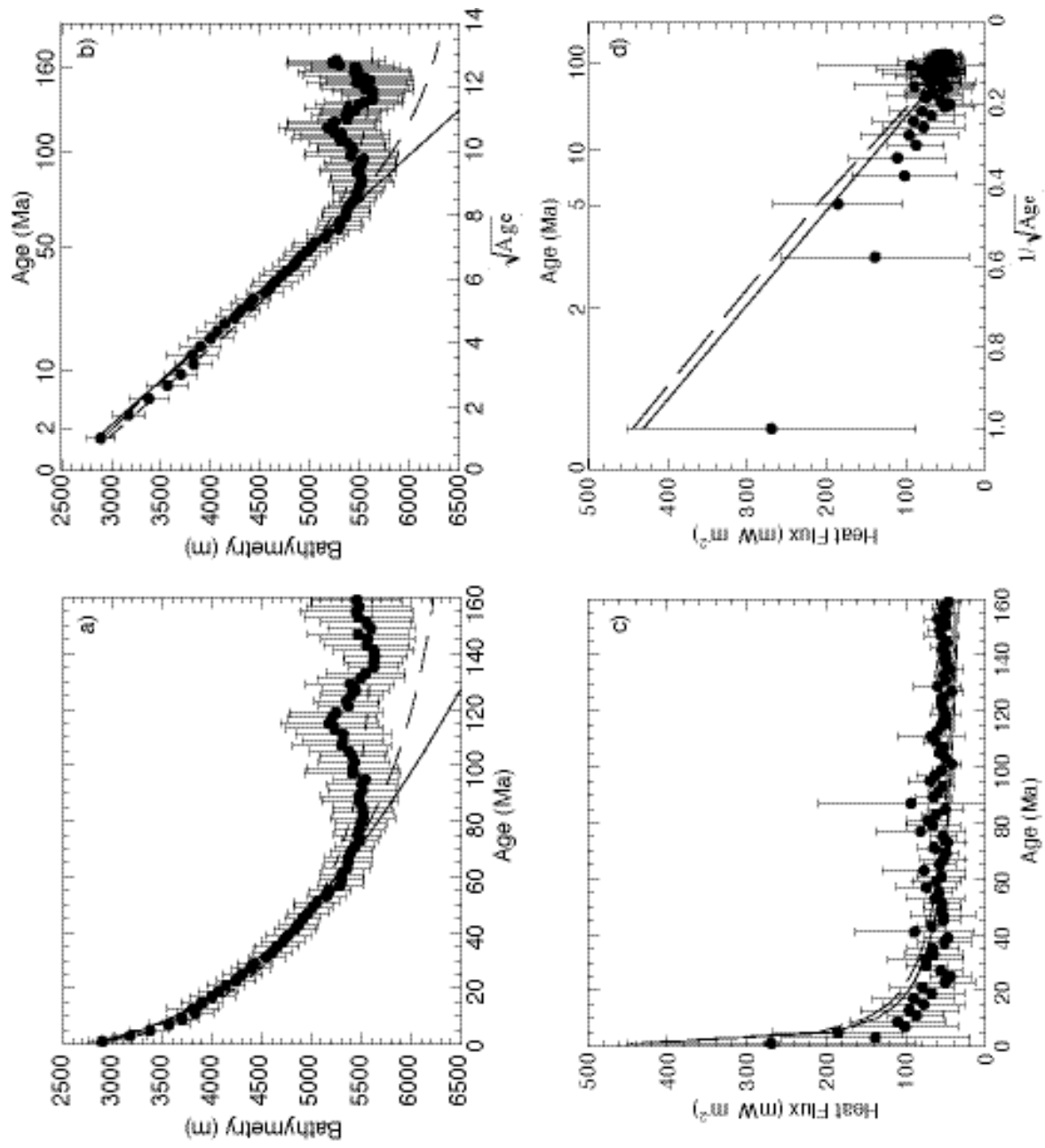


Figure 10.1. Harris and Chapman

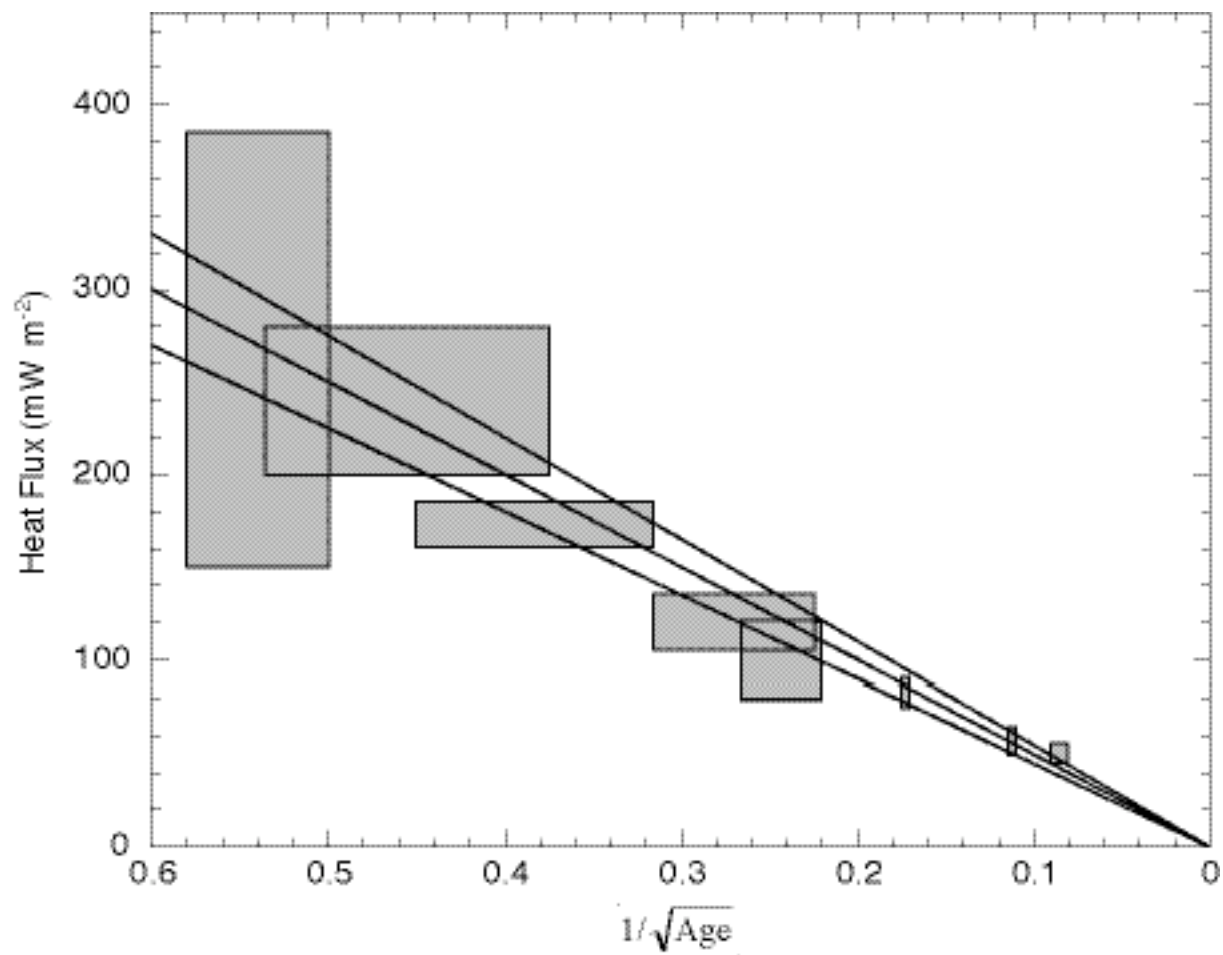


Figure 10.2. Harris and Chapman

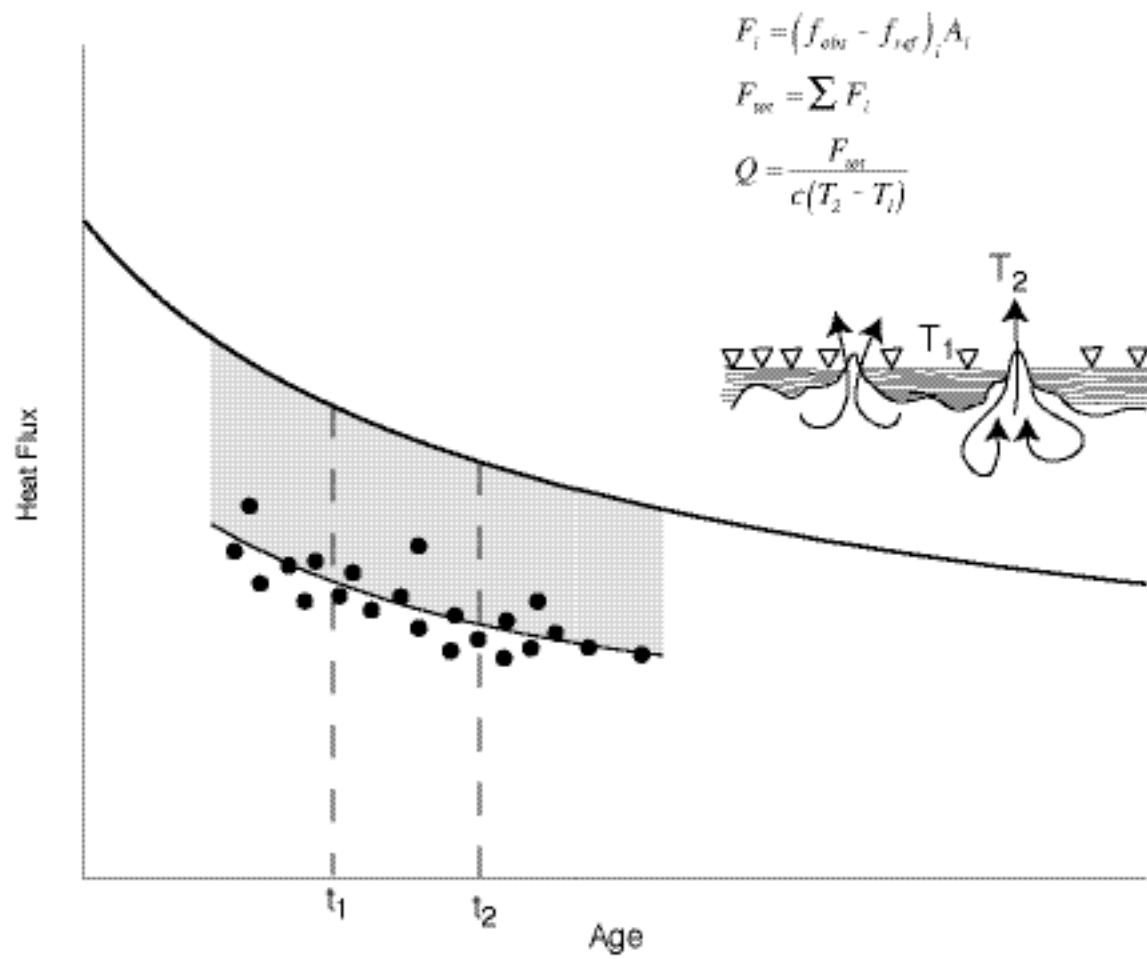


Figure 10.3. Harris and Chapman

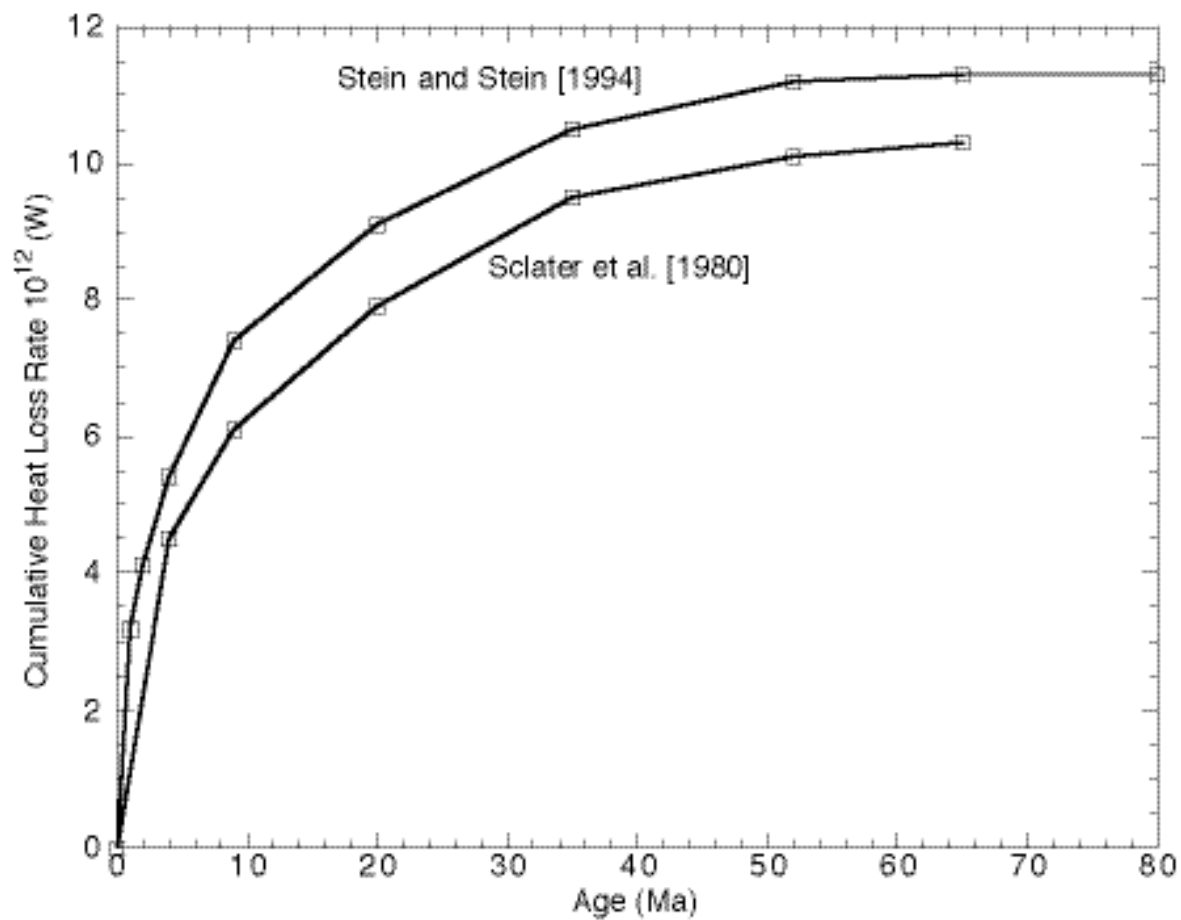


Figure 10.4. Harris and Chapman

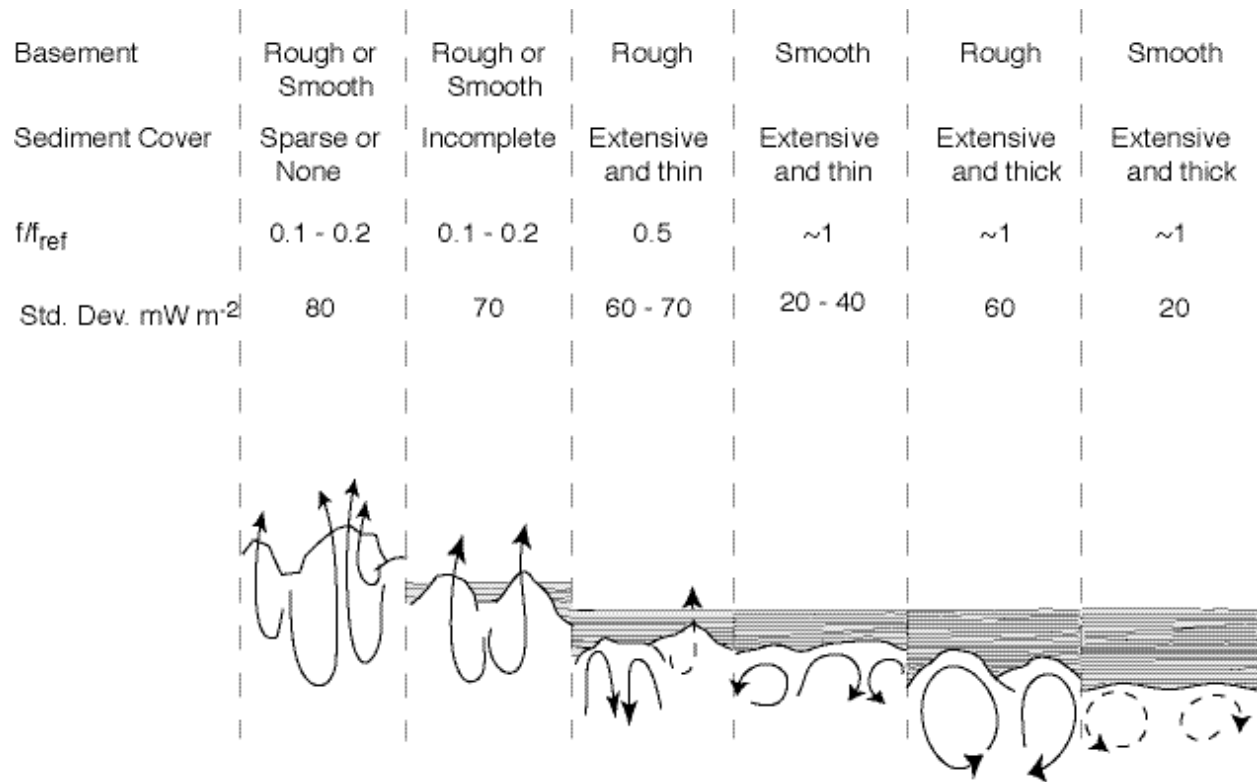


Figure 10.5. Harris and Chapman

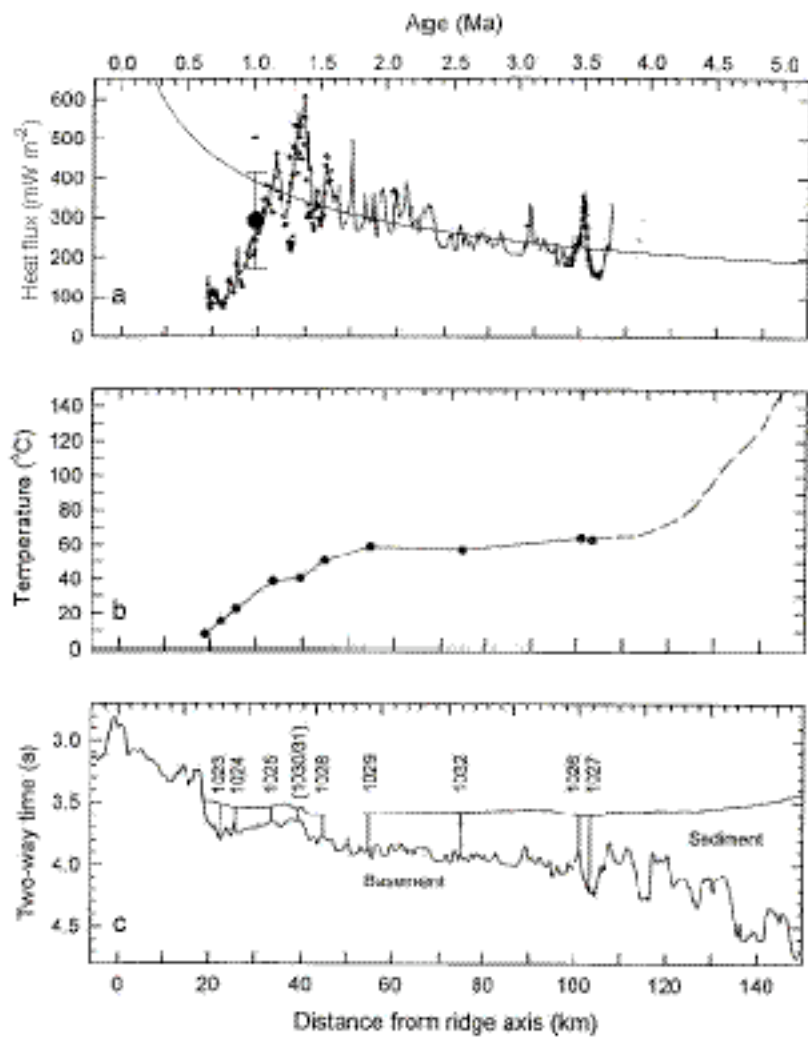


Figure 10.6. Harris and Chapman

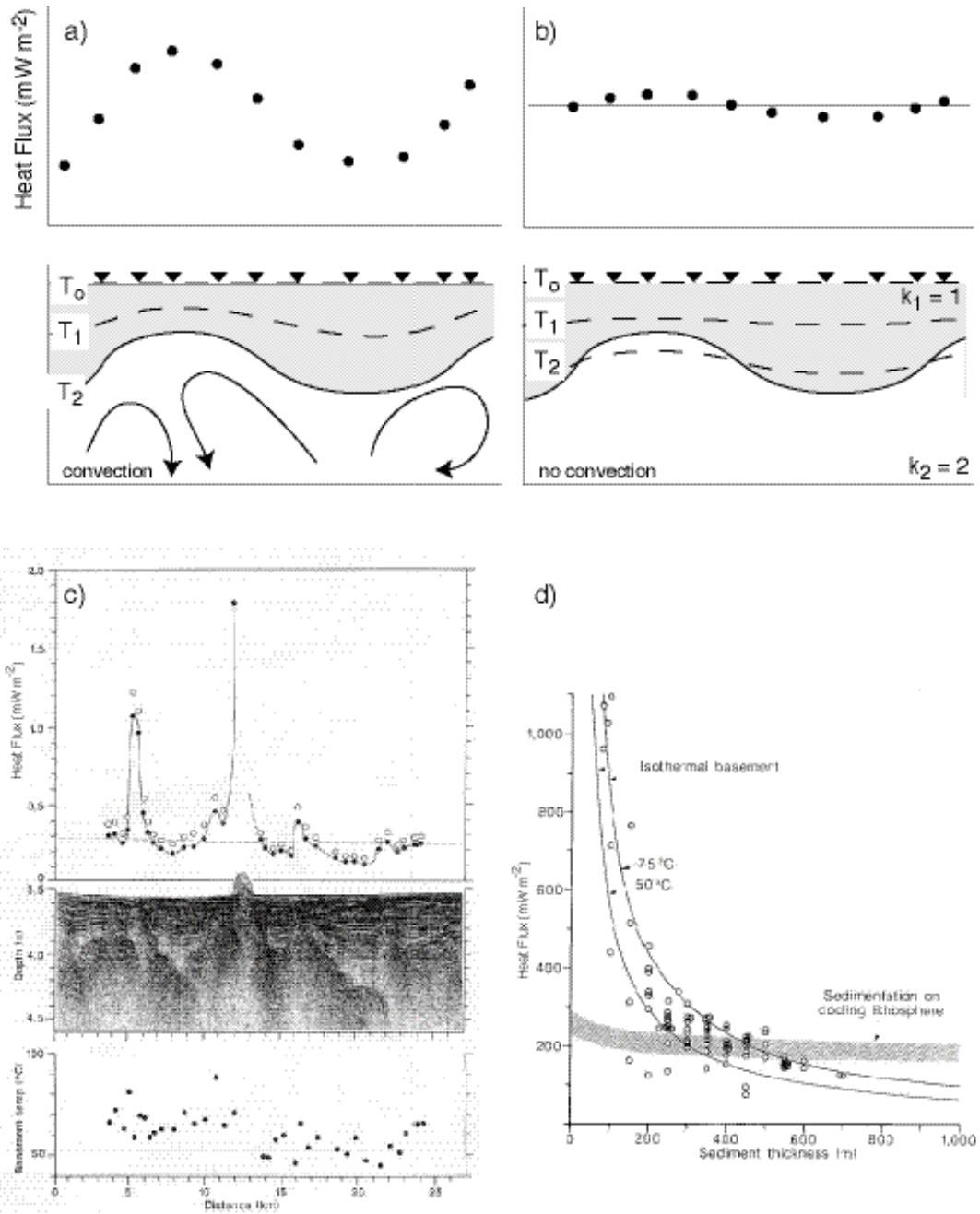


Figure 10.7. Harris and Chapman